Asymmetry of the energy dependence of the charge density wave modulation of $2H$-$NbSe_2$

B. Behmand and C. Lupien*
Department of Physics, Université de Sherbrooke, Sherbrooke, Qc J1K 2R1, Canada.

T. T. M. Palstra
Solid State Chemistry Laboratory, Zernike Institute for Advanced Materials, University of Groningen, Nijenborgh 4, 9747 AG Groningen, The Netherlands
(Dated: October 26, 2009)

Theoretical predictions of unconventional charge density waves (CDW) such as pair density waves have a characteristic symmetry of the energy dependence of the local density of state (LDOS) modulations. The scanning tunneling microscopy (STM) and spectroscopy (STS) techniques obtain information related to the LDOS and could extract the symmetry but setpoint effects prevent a direct identification of the theoretical energy symmetry. We have investigated these effects in the conventional CDW compound $2H$-$NbSe_2$ with very low temperature STM/STS. We observed the expected setpoint effects on the LDOS modulation. The CDW amplitude of $2H$-$NbSe_2$ is mostly asymmetric as expected. The CDW modulation amplitude peaks around 80 meV and is present up to 140 meV. It is very weak below 4 meV. This large energy range for the presence of the CDW modulations needs to be taken into consideration for theoretical models of $2H$-$NbSe_2$.

PACS numbers: 68.37.Ef, 71.45.Lr,74.70.Ad

Strongly correlated systems have phase transitions to many complex orders. One of the possibilities is some density of state modulation such as a charge density wave (CDW). For example, many spatial structures have been observed in the cuprates high temperature superconductors like checkerboards[1], electronic glass[2] and quasiparticle interference[3–6]. There are many theoretical candidates to explains those structures. In particular for the checkerboard there are suggestions of stripes[7] and pair density waves (PDW)[8,9]. For the PDW described in Ref. 8 it is expected that the local density of states (LDOS) modulations $n(E,\mathbf{q})$ be symmetric as a function of energy E, i.e. that $n(E,\mathbf{q}) = n(-E,\mathbf{q})$ for a modulation with a reciprocal space vector of $\mathbf{q}$. This is the opposite result from a conventional CDW where the energy dependence is asymmetric: $n(E,\mathbf{q}) = -n(-E,\mathbf{q})$. Therefore measurements of the symmetry of the energy dependence of the LDOS modulation could provide identification of the proper state.

An obvious technique to use to extract the LDOS symmetry is scanning tunneling spectroscopy (STS). The conductance $g = dI/dV$ measured by the technique, within a certain level of approximation, is proportional to the LDOS. Therefore it is expected that the Fourier transform of a conductance map would yield the symmetry information. However there is an experimental complication that prevents this direct identification. The conductance maps are usually measured while scanning under the constant current condition[10]. In this mode the conductance spectra are normalized at every points of the map to keep the current constant at I_0. This is achieved automatically by a feedback circuit that adjusts the height of the tip above the sample. Since the setpoint current (I_0) is the integral of the conductance from $V = 0$ (Fermi energy) to the setpoint voltage V_0, the measured spatially dependent conductance can be expressed as

$$g(V,\mathbf{r}) = I_0 \frac{n(eV,\mathbf{r})}{\int_0^{V_0} n(eV,\mathbf{r})dV} \tag{1}$$

where e is the charge of the electron to convert the voltages(V) into energies (E) referenced to the Fermi energy. The LDOS is given by $n(E,\mathbf{r})$. This formulation includes the effect of tunneling matrix elements and work function variations within it. However if these additional contributions are independent of the energy, their effect disappears in the normalization since they don't change the shape of the spectra. Otherwise their effect is indistinguishable from an intrinsic LDOS variation.

Assuming Eq. (1) is a good representation of the measured conductance we can now explore the effect of the normalization. We express the LDOS in terms of the Fourier components:

$$\begin{aligned} n(E,\mathbf{r}) =& n_0(E) + n_{k1}(E)e^{i\mathbf{k}_1\cdot\mathbf{r}} + n^*_{k1}(E)e^{-i\mathbf{k}_1\cdot\mathbf{r}} \\ &+ \dots \end{aligned} \tag{2}$$

where n_0 is the $\mathbf{k} = 0$ term, which represents the spatial average of the LDOS, n_{k1} is the complex amplitude of the density modulation with a reciprocal vector of $\mathbf{k}_1$ and we only keep one $\mathbf{k}$ term but many others are present. Using this and dropping the complex conjugate term we express the integral of Eq. (1) as

$$N(\mathbf{r}) = \int_0^{V_0} dV n_0(eV) + n_{k1}(eV)e^{i\mathbf{k}_1\cdot\mathbf{r}} \tag{3}$$

$$= N_0 + N_{k1}e^{i\mathbf{k}_1\cdot\mathbf{r}} \tag{4}$$

where N_0 is the spatial average of the integral and N_{k1} is the complex amplitude of the integral for $\mathbf{k}_1$. Assuming

that $N_k \ll N_0$ for any $k \neq 0$, and keeping only terms to first order we obtain:

$$g(V,\mathbf{r}) = g_0(V) + g_{k1}(V)e^{i\mathbf{k}_1\cdot\mathbf{r}} \quad (5)$$

$$= \frac{I_0}{N_0}\left[n_0(E) + \left(n_{k1}(E) - n_0(E)\frac{N_{k1}}{N_0}\right)e^{i\mathbf{k}_1\cdot\mathbf{r}}\right] \quad (6)$$

where $g_0 = \frac{I_0}{N_0}n_0$ is the spatial average of the conductance and $g_{k1} = \frac{I_0}{N_0}\left(n_{k1}(E) - n_0(E)\frac{N_{k1}}{N_0}\right)$ is the modulation of the conductance at vector $\mathbf{k}_1$. It is obvious from that formulation that the measured g_{k1}, extracted from a Fourier transform of a conductance map is influenced by the normalization. The correction introduced by the setpoint effect effectively shifts the LDOS by a fraction ($\frac{N_{k1}}{N_0}$) of the spatially averaged LDOS n_0. The size of the energy dependent shifts is set to nullify the integral of g_{k1} between $V = 0$ and the setpoint V_0. This is a more general result that is independent of the approximation to keep only first order terms. We have performed the equivalent of integrating the Fourier transform, but if we invert the sequence, i.e. integrate Eq. (1) then take the Fourier transform, it becomes obvious that only the $\mathbf{k} = 0$ component will be non-zero since the integral produces the spatially uniform constant I_0. The consequence is that the $n_0\frac{N_{k1}}{N_0}$ term behaves as an average modulation over the voltage range between $V = 0$ and the setpoint V_0. This also means that the real and imaginary parts of the g_{k1} signal need to cross zero at least once over that same interval. In general it is possible that $N_k = 0$, which would still show at least one zero crossing but it would be intrinsic to the material and not due to the setpoint effect in that case.

The complications introduced by the setpoint normalization for the identification of the symmetry of the LDOS can be better understood if many conductance maps are gathered using different setpoint voltages. In particular, if maps can be taken where $N_k = 0$ and all $n_k(E) = 0$ below the setpoint then the normalization offset would be removed. At the opposite end, if the setpoint is adjusted well outside the energy range of the modulation then N_k remains fix while N_0 increases and this will decrease the importance of the setpoint normalization.

When looking at the region around the Fermi energy, it is quite possible that $n_k \approx 0$ or at least becomes small compared to the setpoint effect. Under these conditions the conductance will have the symmetry of n_0. Since n_0 is often symmetric, this would lead to the wrong conclusion about the energy symmetry of the LDOS modulation. Therefore extreme care needs to be taken when analyzing the raw Fourier amplitudes of conductance map to prevent an erroneous symmetry identification.

Recently many STS experiments have introduced the ratio of conductance maps as a way to increase the contrast of a particular modulation[5,11], to extract a doping dependence[2] and to study the behavior of the bogoliubov superconducting quasi-particles[12]. The ratio Z is given by

$$Z(V,\mathbf{r}) = \frac{g(V,\mathbf{r})}{g(-V,\mathbf{r})}. \quad (7)$$

Using the expression of Eq. (5) and again keeping only terms up to first order this becomes

$$Z(V,\mathbf{r}) = Z_0(V) + Z_{k1}(V)e^{i\mathbf{k}_1\cdot\mathbf{r}} \quad (8)$$

$$= \frac{g_0^+}{g_0^-}\left[1 + \left(\frac{g_{k1}^+}{g_0^+} - \frac{g_{k1}^-}{g_0^-}\right)e^{i\mathbf{k}_1\cdot\mathbf{r}}\right] \quad (9)$$

or in terms of the LDOS

$$Z(V,\mathbf{r}) = \frac{n_0^+}{n_0^-}\left[1 + \left(\frac{n_{k1}^+}{n_0^+} - \frac{n_{k1}^-}{n_0^-}\right)e^{i\mathbf{k}_1\cdot\mathbf{r}}\right], \quad (10)$$

where we introduced the notation $f^+ = f(+E)$ and $f^- = f(-E)$ with $E = eV$ for both the LDOS and the conductance. This ratio therefore becomes $Z = 0$ when both the averaged density of states and the modulated LDOS are purely symmetric, i.e. when $n_0^+ = n_0^-$ and $n_k^+ = n_k^-$. For a n_0 that is not perfectly symmetric the cancellation will no longer be achieved. However when the modulation amplitude is related to the average amplitude, $n_k = n_0(1 + \alpha_k)$, and where $\alpha_k^+ = \alpha_k^-$ then the cancellation is recovered. It is important to remark however that $Z = 0$ does not imply a symmetric LDOS. It can also imply that there is simply no modulation at that energy. Applied to an asymmetric LDOS modulation this ratio extracts amplitude information that is unaffected by the setpoint normalization.

We now proceed to test these concepts in a conventional CDW material. We prepared a crystal of $2H$-$NbSe_2$ by the standard vapor-transport technique. This material has a CDW order at $T_{CDW} = 33.5$ K and a superconducting order at $T_c = 7.2$ K[13]. The crystal structure is hexagonal and the incomensurate CDW has a period of approximately $3a_0$ where $a_0 = 3.45$ Å is the crystal lattice parameter[14]. The mechanism of the CDW in this material has not been understood yet. The nested Fermi surfaces segments associated with a CDW have not been localized and many recent ARPES measurements have identified features probably related to the CDW but at quite different energies[15–18].

Many STM studies have been performed on this material[19–23]. In particular Ref. 23 looked at explaining the setpoint effect in topographic images. The theory suggest that the phase of the modulation changes with energy but that the expected phase shift of 180° that occurs in one-dimensional systems is not present for $2H$-$NbSe_2$. It predicts phase shifts of ±120° instead.

The experiments were carried out in a home built STM installed in a custom design ^{3}He cryostat. The sample was prepared by cleaving inside the cryogenic vacuum at the 4.2 K stage. All the measurements were performed with the microscope at a temperature of 450 mK. The images and maps all had a resolution of 256 by 256 pixels.

In Fig. 1a) we see a large (20 nm) topography taken with a setpoint voltage of -100 mV and current of -100

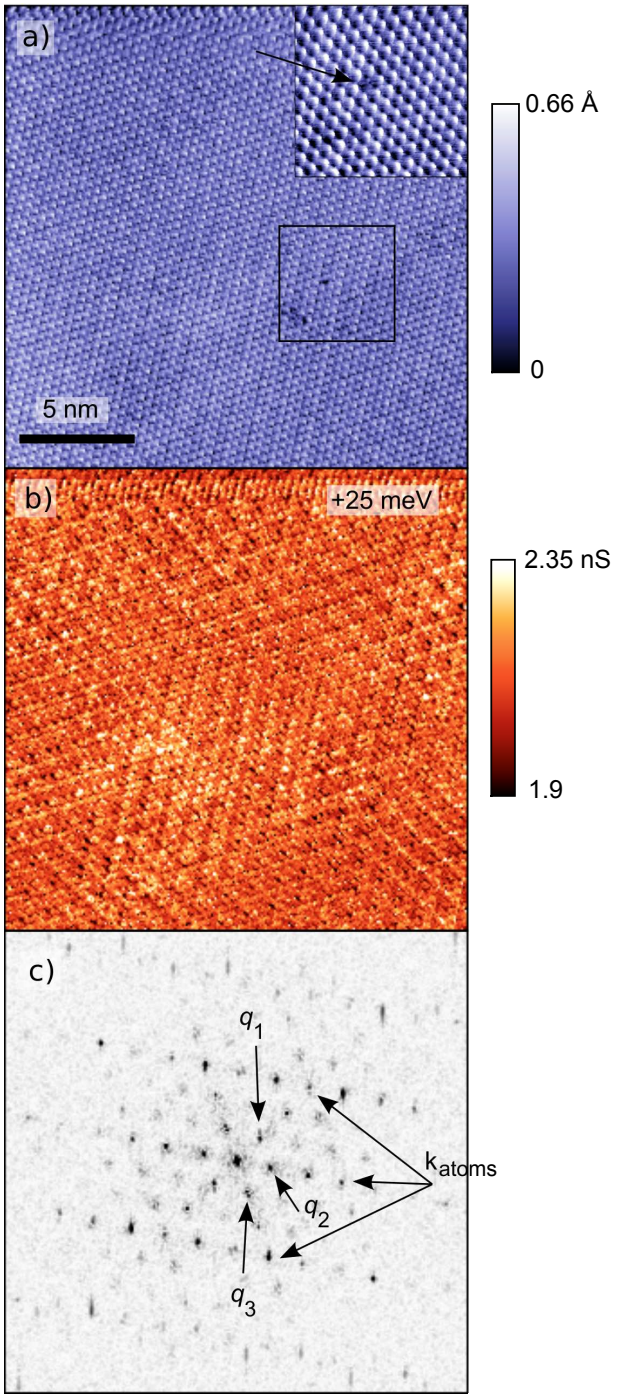

FIG. 1. (Color online) a) Constant current topography of $2H$-$NbSe_2$ over 20 nm. The inset shows a zoom of the region identified by a square and shows a single defect marked by an arrow. b) The +25 meV conductance map taken at the same time as the topography. c) The FFT of the conductance map with the identification of the 3 primary q vectors of the CDW and of the modulation signal due to the atomic crystal lattice.

pA. Most of the other data sets that will be analyzed were measured over a 10 nm area. The weak pattern that modulates the atomic amplitude and that repeats every 3 atoms along the 3 crystal directions is the CDW. The inset presents a zoom of the region where a defect was observed, and shows the system achieved a good atomic resolution. However some tip instability was present and therefore some of the data sets presented later were done under different tip conditions. Nonetheless the qualitative features presented here were independent of the tip condition. The CDW pattern becomes clearer in the conductance map shown in Fig. 1b) which was taken at the same time as the topography. The measurements are done by stopping the feedback at every pixel of the topography and taking a conductance dI/dV spectra directly using a lock-in amplifier technique. Before the feedback is disabled the setpoint is temporarily modified to $V_0 = -100$ mV and $I_0 = -300$ pA to improve the conductance signal. A modulation amplitude of 5 mV_{RMS} was added to the sample voltage for the lock-in technique. Finally Fig. 1c) shows the fast Fourier transform (FFT) of the conductance map. With arrows we identify the modulation signal produced by the atomic structure and the three primary $\mathbf{q}$ vectors produced by the CDW. We obtain that $|k_{atoms}/q| = 3.1 \pm 0.1$ as expected.

We now extract the values of the FFT at the origin ($\mathbf{k} = 0$) and at the primary vectors of the CDW and obtain Fig. 2. The conductance map used for this analysis is not the one from Fig. 1. It used a setpoint of $V_0 = -140$ mV with a modulation amplitude of 5 mV_{RMS}. Fig. 2a) shows the $\mathbf{q} = 0$ component which is the spatial average of the conductance. A weak energy asymmetry of about 0.8 is displayed in the curve when comparing positive sample voltages with the negative ones. With the modulation amplitude used here the superconducting gap is not observable. Around ±30 mV there is a decrease in the conductance. This was originally identified as the CDW gap[19,20] but recent ARPES measurements suggest the feature might be a saddle point singularity instead[15]. In Fig. 2b) and c) we see the real and imaginary parts of the FFT at the three primary CDW $\mathbf{q}$ vectors. To improve the clarity of the figure we have fixed the phase of the g_q to be purely real at -140 mV[24]. As expected the curves cross zero between the setpoint voltage and the Fermi energy. If both n_0 and n_q were symmetric we would expect a symmetric g_q. But here the g_qs are not symmetric, even considering the imperfect symmetry of g_0. They are not purely asymmetric either but that is expected from the setpoint normalization effect and from the phase jumps that are expected to be different than 180°. The peak in g_{q2} at $V = 0$ (and to a lesser extent in g_{q3}) is not present in all the data sets and is not understood. However it is restricted to a small energy around $V = 0$ (the voltage modulation is 5mV_{RMS}) since the zero crossing does not seem to be affected strongly by its presence. Later we will show results from a conductance map taken over that small energy range.

To observe the effect of the setpoint we also display

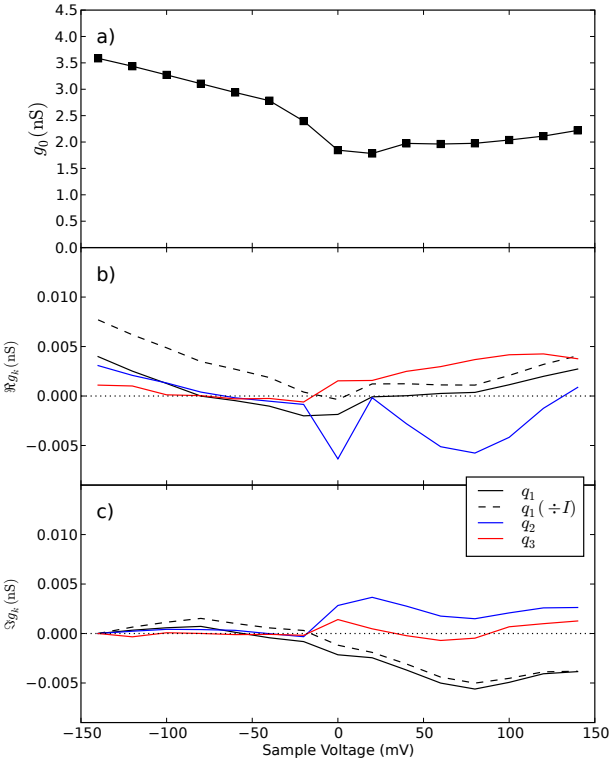

FIG. 2. (Color online) a) The square are the amplitude of the $\mathbf{k} = 0$ point from the FFT of a conductance map. The lines are a guide to the eye. b) and c) show respectively the real and imaginary parts at the three $\mathbf{q}$ vectors of the CDW from the same FFT. The setpoint was $V_0 = -140$ mV and $I_0 = -420$ pA, and all the solid curves cross zero on the negative side around -70 mV. The dashed line is obtained after renormalizing the map to a setpoint of $V_0 = -40$ mV (as described in the text) and crosses the origin much closer to 0 mV. For display purposes the phase of the q signal was forced to be purely real at -140 mV.

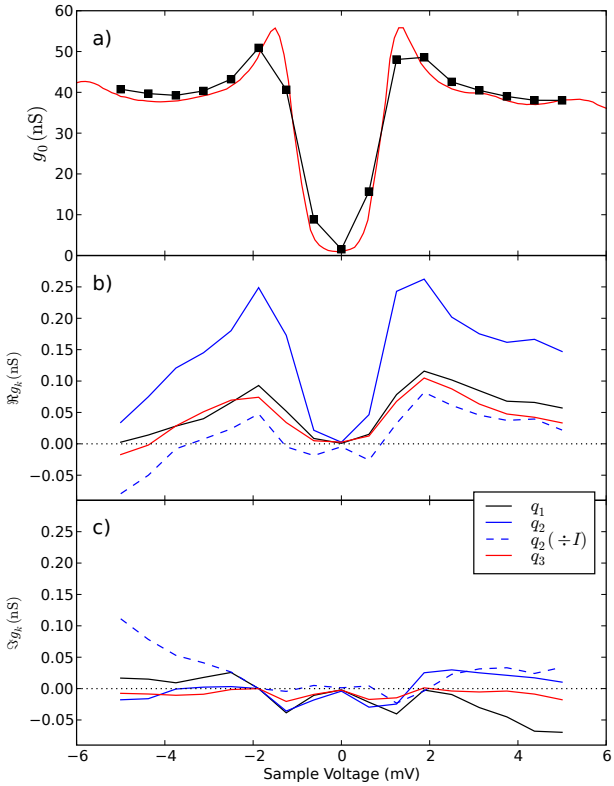

FIG. 3. (Color online) The same as for Fig. 2 except the energy range is ±5 meV, and the curves are forced to be real at −1.9 mV. The setpoint conditions were $V_0 = -20$ mV, $I_0 = -800$ pA and a modulation amplitude of 0.4 $\mathrm{mV_{RMS}}$ was used. The red curve in a) is an averaged point spectra using a modulation amplitude of 70 $\mu\mathrm{V_{RMS}}$. The renormalized curve (dashed) used a new setpoint of −1.9 mV.

data obtained for a different voltage setpoint of $V_0 = -40$ mV as the dashed line. Here the crossing is moved closer to the Fermi energy and the curves are modified by almost a constant shift which is expected since g_0 is roughly flat. This data was not obtained from a separate conductance map but was simulated from the $V_0 = -140$ mV conductance map. This was achieved by measuring the current map $I(V, \mathbf{r})$ at the same time as the conductance map. With this additional information we can simulate a new map g' under a different setpoint V_0' condition by

$$g'(V, \mathbf{r}) = g(V, \mathbf{r}) \frac{\overline{I}(V_0')}{I(V_0', \mathbf{r})} \tag{11}$$

where $V_0' = -40$ mV is the new setpoint and $\overline{I}$ is the spatially average current over the map. At the level of approximations used above in Eq. (1) this should have the same result as measuring a new conductance map under a different setpoint. We qualitatively checked and confirmed that the same results are obtained with a measured map compared to a simulated map.

In Fig. 3 we see the same measurement as in Fig. 2 but for a smaller energy range around the superconducting transition. The superconducting gap is clearly visible. The fact the setpoint voltage was set at -20 mV explains why almost no zero crossing is seen in Fig. 3b) and c). Over this energy range g_0 is very symmetric. The g_qs curves are also quite symmetric. This can be explained by a symmetric density wave like a PDW but it could also simply be the result of the setpoint effect with a weak or absent asymmetric signal at these energies. The renormalized dashed curve ($V_0' = -1.9$ mV) shows that much less signal is present and it has become less symmetric. Therefore between ±4 mv only a very weak CDW signal is present. Hence the original $V_0 = -20$ mV signal was misleading.

Another aspect of this asymmetry can be extracted from the FFT of the Z ratio. In Fig. 4 we analyze the same map as in Fig. 2. To correctly understand the amplitude of Z we need a reference scale for comparison. In particular, for the case of a symmetric signal where we expect $Z = 0$, we need to know how good the zero is.

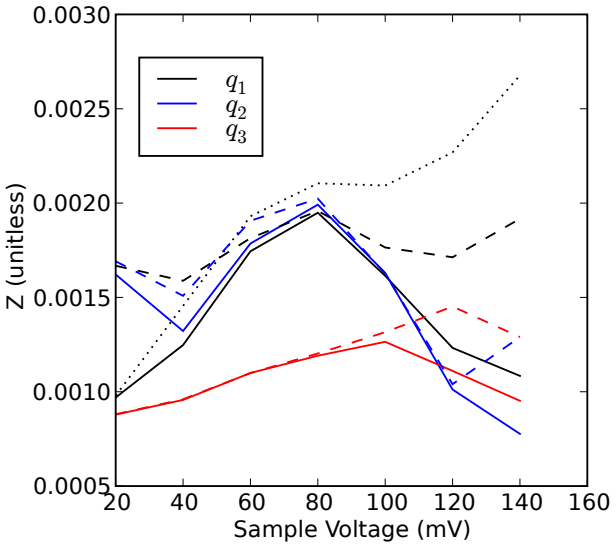

FIG. 4. (Color online) Using the same map as for Fig. 2 we display Z (solid lines) and $Z_{\max}$ (dashed line) for the 3 principal $\mathbf{q}$ vectors of the CDW. The dotted line is $Z_{\max}$ for the data renormalized with $V_0' = -40$ mV. The proximity between Z and $Z_{\max}$ suggests a mostly asymmetric CDW. The CDW signal is present at all energies but seems to be decreasing above 100 mV.

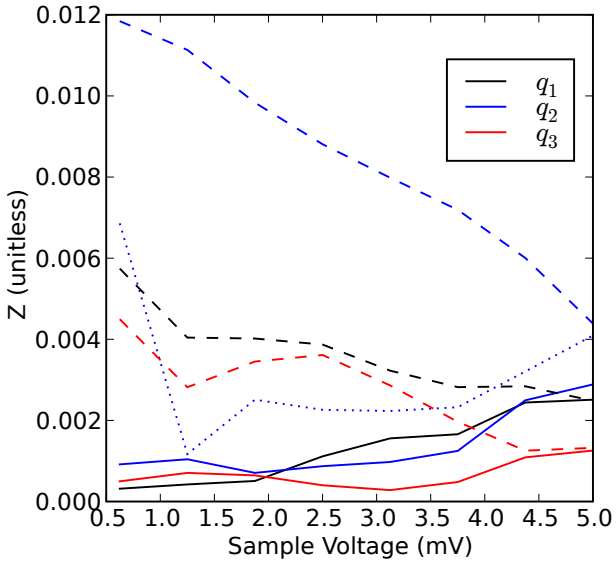

FIG. 5. (Color online) Using the same map as for Fig. 3 we display Z (solid lines) and $Z_{\max}$ (dashed line) for the 3 principal $\mathbf{q}$ vectors of the CDW. The dotted line is $Z_{\max}$ for the data renormalized with $V_0' = -1.9$ mV. Since Z and $Z_{\max}$ are separated this suggests no CDW signal. It could also signify the presence of a symmetric density wave, but the renormalized curve is inconsistent with that identification.

Therefore we also plot $Z_{\max}$ which is obtained as

$$Z_{\max}(V,q) = \frac{g_0^+}{g_0^-} \times \sqrt{\left(\left|\frac{\Re g_q^+}{g_0^+}\right| + \left|\frac{\Re g_q^-}{g_0^-}\right|\right)^2 + \left(\left|\frac{\Im g_q^+}{g_0^+}\right| + \left|\frac{\Im g_q^-}{g_0^-}\right|\right)^2} \quad (12)$$

where this expression considers the signal as purely asymmetric and handle the imaginary and real part separately. This will provide a maximum value for Z irrespective of the symmetry. However some care needs to be taken with this expression. When either g_q^+ or g_q^- is zero this expression reduces to Z itself so it not useful at those energies. Another point to be keep in mind is that $Z_{\max}$ includes the effect of the setpoint normalization. Therefore if n_q becomes small, $Z_{\max}$ will stay stuck with a value dependent on $n_0 \frac{N_q}{N_0}$.

In Fig. 4 we see that Z and $Z_{\max}$ are close. As expected they become almost equal at the zero crossing voltage of Fig. 2. The renormalized setpoint (dotted) $Z_{\max}$ curve, is quite different from the original one (black dashed) but there is a unique Z curve for both. This large variation in $Z_{\max}$ shows that care is needed when using it. Nonetheless, for a purely symmetric density wave, we expect $Z_{\max}$ to be well above $Z \approx 0$ irrespective of the setpoint and this is obviously not the case here. After peaking around 80 mV, all the Z curves are decreasing above 100 mV and they tend to separate from $Z_{\max}$ (note that g_{q2} has a zero around +130 V which makes $Z_{\max} \approx Z$). The modulation signal coming from the CDW is therefore present at all the energies presented here but it tends to disappear at the higher energies. This result is consistent with recent ARPES measurements[18] where changes in the spectral weight were observed over a large range of energies. The effect of the CDW in $2H$-$NbSe_2$ does not seem restricted to a small region around the Fermi energy.

Finally, for the low energy map, the result of the Z analysis are displayed in Fig. 5. Here Z and $Z_{\max}$ are quite separated, especially at low energy. This suggests a symmetric signal, or a small asymmetric signal with $Z_{\max}$ influenced by the setpoint effect. We see the later is the probable because the renormalized $Z_{\max}$ (dashed curve) is much lower and this is consistent with the analysis of Fig. 3 above. Therefore the CDW modulation is very weak or simply absent at energies below 4 meV.

In conclusion, we described some techniques to allow the analysis of the symmetry of LDOS modulation using STM that consider the important effect of setpoint normalization. We applied those techniques to the conventional CDW material $2H$-$NbSe_2$. As expected, we obtained that the CDW is mostly asymmetric. We also observed that the CDW is present over a large range of energies (up to 140 meV) peaking around 80 meV but is mostly absent at low energies (below 4 meV). This is consistent with the recent ARPES results of Ref. 18 and has important implications for the theories of the CDW in this material. Further STS measurements are needed to more precisely identify the CDW energy range and its relation to the superconducting energy gap.

ACKNOWLEDGMENTS

We acknowledge funding from NSERC of Canada and FQRNT of Quebec.

---

* Author to whom correspondence should be addressed: Christian.Lupien@USherbrooke.ca

[1] T. Hanaguri, C. Lupien, Y. Kohsaka, D. Lee, M. Azuma, M. Takano, H. Takagi, and J. Davis, Nature (London) **430**, 1001 (Aug 26 2004).

[2] Y. Kohsaka, C. Taylor, K. Fujita, A. Schmidt, C. Lupien, T. Hanaguri, M. Azuma, M. Takano, H. Eisaki, H. Takagi, S. Uchida, and J. C. Davis, Science **315**, 1380 (Mar 9 2007).

[3] K. McElroy, R. Simmonds, J. Hoffman, D. Lee, J. Orenstein, H. Eisaki, S. Uchida, and J. Davis, Nature (London) **422**, 592 (Apr 10 2003).

[4] M. Vershinin, S. Misra, S. Ono, Y. Abe, Y. Ando, and A. Yazdani, Science **303**, 1995 (Mar 26 2004).

[5] Y. Kohsaka, C. Taylor, P. Wahl, A. Schmidt, J. Lee, K. Fujita, J. W. Alldredge, K. McElroy, J. Lee, H. Eisaki, S. Uchida, D. H. Lee, and J. C. Davis, Nature (London) **454**, 1072 (Aug 28 2008).

[6] W. D. Wise, K. Chatterjee, M. C. Boyer, T. Kondo, T. Takeuchi, H. Ikuta, Z. Xu, J. Wen, G. D. Gu, Y. Wang, and E. W. Hudson, Nat. Phys. **5**, 213 (Mar 2009).

[7] E. Berg, E. Fradkin, and S. A. Kivelson, Phys. Rev. B **79**, 064515 (2009).

[8] H.-D. Chen, O. Vafek, A. Yazdani, and S.-C. Zhang, Phys. Rev. Lett. **93**, 187002 (Oct 2004).

[9] E. Berg, Erez amd Fradkin and S. A. Kivelson, Nat. Phys.(Sept 2009), doi:\bibinfo{doi}{10.1038/nphys1389}.

[10] A single map can last 24 hours which makes the constant height mode very difficult since it requires compensating for piezo drift accurately over long periods of time.

[11] T. Hanaguri, Y. Kohsaka, J. C. Davis, C. Lupien, I. Yamada, M. Azuma, M. Takano, K. Ohishi, M. Ono, and H. Takagi, Nat. Phys. **3**, 865 (Dec 2007).

[12] K. Fujita, I. Grigorenko, J. Lee, W. Wang, J. X. Zhu, J. C. Davis, H. Eisaki, S. Uchida, and A. V. Balatsky, Phys. Rev. B **78**, 054510 (2008).

[13] A. Gabovich, A. Voitenko, J. Annett, and M. Ausloos, Supercond. Sci. Technol. **14**, R1 (Apr 2001).

[14] D. E. Moncton, J. D. Axe, and F. J. DiSalvo, Phys. Rev. B **16**, 801 (Jul 1977).

[15] S. V. Borisenko, A. A. Kordyuk, V. B. Zabolotnyy, D. S. Inosov, D. Evtushinsky, B. Büchner, A. N. Yaresko, A. Varykhalov, R. Follath, W. Eberhardt, L. Patthey, and H. Berger, Phys. Rev. Lett. **102**, 166402 (2009).

[16] T. Kiss, T. Yokoya, A. Chainani, S. Shin, T. Hanaguri, M. Nohara, and H. Takagi, Nat. Phys. **3**, 720 (Oct 2007).

[17] T. Valla, A. V. Fedorov, P. D. Johnson, P.-A. Glans, C. McGuinness, K. E. Smith, E. Y. Andrei, and H. Berger, Phys. Rev. Lett. **92**, 086401 (Feb 2004).

[18] D. W. Shen, Y. Zhang, L. X. Yang, J. Wei, H. W. Ou, J. K. Dong, B. P. Xie, C. He, J. F. Zhao, B. Zhou, M. Arita, K. Shimada, H. Namatame, M. Taniguchi, J. Shi, and D. L. Feng, Phys. Rev. Lett. **101**, 226406 (2008).

[19] C. Wang, B. Giambattista, C. G. Slough, R. V. Coleman, and M. A. Subramanian, Phys. Rev. B **42**, 8890 (Nov 1990).

[20] Z. Dai, Q. Xue, Y. Gong, C. G. Slough, and R. V. Coleman, Phys. Rev. B **48**, 14543 (Nov 1993).

[21] I. Guillamon, H. Suderow, F. Guinea, and S. Vieira, Phys. Rev. B **77**, 134505 (2008).

[22] B. Giambattista, A. Johnson, R. V. Coleman, B. Drake, and P. K. Hansma, Phys. Rev. B **37**, 2741 (Feb 1988).

[23] W. Sacks, D. Roditchev, and J. Klein, Phys. Rev. B **57**, 13118 (May 1998).

[24] The complex amplitude that is displayed (A') is converted from the raw amplitude (A) by $A'(V) = A(V)\frac{|A(V_r)|}{A(V_r)}$ with V_r the energy where the amplitude becomes purely real.